Journal of Applied Mathematics & Bioinformatics, vol.4, no.3, 2014, 1-28
ISSN: 1792-6602 (print), 1792-6939 (online)
Scienpress Ltd, 2014

MHD Pulsatile Slip Flow Of Blood Through Porous Medium In An Inclined Stenosed Artery In Presence Of Body Acceleration

N. Ahmed[1], D. P. Barua[2] and D. J. Bhattacharyya[3]

Abstract

In the present Paper, the Authors have investigated the pulsatile flow of blood through a porous medium with constant permeability, in an inclined artery with mild stenosis. The flow of blood is considered to be Newtonian. The presence of an azimuthal uniform magnetic field is assumed. The flow takes place under body acceleration and a slip velocity is imposed at the stenosed arterial wall. By using Perturbation technique, the solutions for the flow field, wall shear stress, volumetric flux and the effective viscosity are obtained and their behaviours under the influence of various relevant parameters concerning the magnetic field, velocity slip, permeability, inclination etc. have been demonstrated pictorially and

[1] Department of Mathematics, Gauhati University, Guwahati-781014. Assam, India.
E-mail: saheel_nazib@yahoo.com
[2] Department of Mathematics, Gauhati University. E-mail: math_byte@yahoo.com
[3] Department of Mathematics, Gauhati University. E-mail: shandilyadhruva@gmail.com

Article Info: *Received* : June 1, 2014. *Revised* : June 29, 2014.
Published online : October 15, 2014.

discussed. It is seen that the applied magnetic field, velocity slip, inclination and the permeability of the porous medium have significant influence on the flow field, wall shear stress, volumetric flow rate and the effective viscosity.

Mathematics Subject Classification: 76Z05; 74G10; 76W05
Keywords: MHD; Pulsatile; Porous; Slip velocity; Blood flow; Stenosis; Inclined

1 Introduction

The studies related to blood flow through stenosed arteries have garnered wide interest in the field of Bio-Medical research. Stenosis or atherosclerosis may be defined as the formation of some constriction in the inner arterial wall owing to the deposition of lipoproteins and fatty acids (atherosclerotic plaques) in the lumen of the artery. Such constrictions lead to considerable change in the flow of blood, the pressure distribution and the wall shear stress, thereby impeding the normal circulatory processes and consequently leading to cardiovascular diseases. Even for mild atherosclerosis, the velocity gradient in the stenosed wall is steep owing to the increased core velocity. This results in comparatively large shear stress on the arterial wall. Mathematical models of blood flow through arteries under diverse physiological situations were presented by several authors like Fung [1], McDonald [2], Zamir [3] and David et al. [4]. Theoretical and experimental investigations concerning flow of blood through stenosed arteries were presented by Young [5], Liu et al. [6], Yao and Li [7] and Mekheimer and El-Kot [8]. The human body may be subjected to body accelerations (vibrations) under certain situations such as riding a heavy vehicle or flying in a helicopter. This may cause health problems like vascular disorders and increased pulse rate. Studies related to blood flow under the influence of body acceleration were carried out by several research workers such as Sud and Sekhon [9] and El-Shahed [10]. The Pulsatile nature of blood flow in arteries may be attributed to the heart pulse pressure

gradient. Studies in pulsatile blood flow were carried out by researchers like [10] and Elshehawey et al. [11]. The possibility of velocity slip at the blood vessel wall was investigated theoretically by Brunn [12] and Jones [13] and experimentally by Bennet [14] and Bugliarello and Hayden [15]. The methods to detect and determine slip experimentally at the blood vessel wall have been indicated by Astarita et al. [16] and Cheng [17] respectively. It was first Kolin [18] and later Korchevskii and Marochnik [19] who suggested the scope of electromagnetic fields in Bio-Medical studies. Barnothy [20] indicated that for biological systems, the heart rate decreases under the influence of an external magnetic field. In certain pathological circumstances, the distribution of fatty cholesterol and artery-clogging blood clots in the lumen of the coronary artery may be regarded as equivalent to a fictitious porous medium. Xu et al. [21] assumed the blood clot as a porous medium to investigate the transport characteristics of blood flow in the extension of multi-scale model by incorporating a detailed sub model of surface-mediated control of blood coagulation (Xu et al. [22, 23]). In general, blood is a non-Newtonian fluid. However, it has been established that human blood exhibits Newtonian behavior at all rates of shear for hematocrits up to about 12% [24]. Further, in case of relatively larger blood vessels it is sensible to assume that blood has a constant viscosity, since the diameters of such vessels are large compared with the individual cell diameters and because shear rates are quite high for viscosity to be independent of them. Consequently, for such vessels the non-Newtonian character becomes unimportant and blood may be regarded as a Newtonian fluid.

In view of the aforementioned facts, we may cite the works done by Elshehawey et al. [11], Nagarani and Sarojamma [25], Shehawey and EL Sebaei [26], Tzirtzilakis [27], etc.

The aim of the present study is to investigate theoretically the nature of a pulsatile blood flow through a mildly stenosed artery under the combined influence of an azimuthal uniform magnetic field, slip velocity, body acceleration

and permeability, when the artery is inclined to the vertical. The investigation is carried out by treating blood flow as Newtonian.

2 The formulation of the Problem

For the present problem, we consider an axially symmetric, laminar, one-dimensional and fully developed flow of blood, through an inclined and constricted circular artery, in the presence of a time-dependent pressure gradient, body acceleration and a uniform circular (azimuthal) magnetic field of moderate intensity. Thus, the induced magnetic field is negligible. We assume that this constricted artery has a rigid wall and that the artery is filled with a porous medium of constant permeability. Further, the artery is inclined to the vertical and a slip velocity is imposed at the stenosed region of the arterial wall. Here, blood is assumed as a Newtonian fluid and the corresponding flow is considered to be Newtonian. The flow configuration is presented pictorially, in the section for figures.

Following Nagarani and Sarojamma [25], the geometry of an arterial stenosis is presented as:

$$\bar{R}\left(\bar{z}\right)=\begin{cases}\bar{L}-\dfrac{\bar{d}_s}{2}\left(1+\cos\dfrac{\pi\bar{z}}{\bar{d}_0}\right), & \text{for } \left|\bar{z}\right|\le\bar{d}_0\\ \bar{L}, & \text{for } \left|\bar{z}\right|>\bar{d}_0\end{cases} \tag{1}$$

Where $\bar{R}\left(\bar{z}\right)$ is the radius of the artery in the stenosed region, $\bar{L}$ is the constant arterial radius in the non-stenosed region, $\bar{d}_0$ is the half-length of the stenosis and $\bar{d}_s$ is the greatest height of the stenosis such that $\dfrac{\bar{d}_s}{\bar{L}}$ is less than unity for a mild stenosis. For a low Reynolds number flow through an artery with mild stenosis, we may omit the radial velocity since it is very small (Nagarani and

Sarojamma [25]).

In cylindrical coordinate system $\left(\bar{r},\bar{\theta},\bar{z}\right)$, the momentum equation governing the flow is deduced from Navier-Stokes equations of motion and presented as under:

$$\frac{\partial \bar{u}}{\partial \bar{t}}=\frac{1}{\rho}\overline{F}\left(\bar{t}\right)+g\cos\beta-\frac{1}{\rho}\frac{\partial \overline{P}}{\partial \bar{z}}+\upsilon\left(\frac{\partial^2 \bar{u}}{\partial \bar{r}^2}+\frac{1}{\bar{r}}\frac{\partial \bar{u}}{\partial \bar{r}}\right)-\frac{\sigma \bar{u}\overline{B}^2}{\rho}-\frac{\upsilon \bar{u}}{\overline{K}} \tag{2}$$

$$\frac{\partial \overline{P}}{\partial \bar{r}}=0 \tag{3}$$

Where $\bar{u}$ denotes the velocity along the $\bar{z}$- axis, $\overline{P}$ the pressure, ρ the density, $\bar{t}$ the time, $\overline{F}\left(\bar{t}\right)$ the body acceleration, $\overline{B}$ the applied magnetic field in azimuthal ($\bar{\theta}$) direction, υ the kinematic viscosity, σ the electrical conductivity, g the acceleration due to gravity, β the angle of inclination of the artery with the vertical and $\overline{K}$ the permeability of the porous medium.

The relevant boundary conditions are as under:

$$\bar{u}=\overline{V_s} \text{ at } \bar{r}=\overline{R}\left(\bar{z}\right) \tag{4}$$

$$\frac{\partial \bar{u}}{\partial \bar{r}}=0 \text{ at } \bar{r}=0 \tag{5}$$

Where $\overline{V_s}$ is the slip velocity at the stenosed region of the arterial wall.

When $\bar{t}>0,$ periodic body acceleration $\overline{F}\left(\bar{t}\right)$ is imposed on the flow and this may be presented as under (Nagarani and Sarojamma [25]):

$$\overline{F}\left(\bar{t}\right)=f_0\cos\left(\overline{\omega}_0\bar{t}+\theta\right), \tag{6}$$

Where $\overline{\omega}_0=2\pi\overline{F_b}$, f_0 and $\overline{F_b}$ being respectively the amplitude of body acceleration and frequency (in Hertz) of body acceleration. Also, θ is the lead angle with respect to the heart action. $\overline{F_b}$ is taken to be so small that wave effect

may be omitted (Nagarani and Sarojamma [25]).

Further, for $\bar{t} \geq 0$, the pressure gradient is assumed as:

$$-\frac{\partial \bar{P}\left(\bar{z},\bar{t}\right)}{\partial \bar{z}} = P_0\left(\bar{z}\right) + P_1\left(\bar{z}\right)\cos\left(\bar{\omega}_P \bar{t}\right) \tag{7}$$

Where $P_0\left(\bar{z}\right)$, $P_1\left(\bar{z}\right)$ are respectively the steady state pressure gradient and the amplitude of the oscillatory part of the pressure gradient. Further, $\bar{\omega}_P = 2\pi \bar{f}_P$ where $\bar{f}_P$ is the pulse rate frequency.

We make the following non-dimensional substitutions:

$$\begin{aligned}
&z = \frac{\bar{z}}{\bar{L}}, R\left(z\right) = \frac{\bar{R}\left(\bar{z}\right)}{\bar{L}}, r = \frac{\bar{r}}{\bar{L}}, t = \bar{t}\,\bar{\omega}_P, \omega = \frac{\bar{\omega}_0}{\bar{\omega}_P}, d_s = \frac{\bar{d}_s}{\bar{L}}, u = \frac{4\upsilon\rho\bar{u}}{P_0\bar{L}^2},\\
&B' = \frac{\rho g}{P_0}, V_s = \frac{4\upsilon\rho\bar{V}_s}{P_0\bar{L}^2}, \tau = \frac{2\bar{\tau}}{P_0\bar{L}}, \varepsilon^2 = \frac{\bar{L}^2\bar{\omega}_P}{\upsilon}, \varepsilon_0 = \frac{P_1}{P_0}, B = \frac{f_0}{P_0},\\
&M = \frac{\sigma\bar{B}^2\bar{L}^2}{\upsilon\rho}, K = \frac{\bar{K}}{\bar{L}^2}, d_0 = \frac{\bar{d}_0}{\bar{L}}, \mu_E = \frac{\bar{\mu}_E}{8\upsilon\rho},
\end{aligned} \tag{8}$$

Where ε, M, K and d_s are respectively the Pulsatile Reynolds number or the Womersley frequency parameter, Hartmann number or magnetic parameter, the permeability parameter and the dimensionless height of the stenosis. The remaining quantities relevant to this problem are described at their appropriate places.

We substitute the quantities defined in (8) into (1), (2), (4), (5), (6) and (7) and then simplifying, we get the following in non-dimensional forms:

Non-dimensional form of the geometry of arterial stenosis is:

$$R\left(z\right) = \begin{cases} 1 - \dfrac{d_s}{2}\left(1 + \cos\dfrac{\pi z}{d_0}\right), & \text{for } |z| \leq d_0 \\ 1, & \text{for } |z| > d_0 \end{cases} \tag{9}$$

Momentum equation:

$$\varepsilon^2 \frac{\partial u}{\partial t} = 4\left\{B\cos\left(\omega t+\theta\right)+B'\cos\beta+\left(1+\varepsilon_0\cos t\right)\right\} + \frac{1}{r}\frac{\partial}{\partial r}\left(r\frac{\partial u}{\partial r}\right)-\left(M+\frac{1}{K}\right)u \tag{10}$$

Subject to the following non-dimensional boundary conditions:

$$u = V_s \text{ at } r = R \tag{11}$$

$$\frac{\partial u}{\partial r} = 0 \text{ at } r = 0 \tag{12}$$

3 Method of Solution

Assuming the Pulsatile Reynolds number ε to be very small, the velocity u may be approximated by the following series (perturbation technique):

$$u\left(z,r,t\right) = v_0\left(z,r,t\right)+\varepsilon^2 v_1\left(z,r,t\right)+..... \tag{13}$$

Substituting (13) in (10), (11) and (12) and equating the coefficients of ε^0 and ε^2 and then neglecting the terms containing higher powers of ε, we obtain:

$$0 = 4h\left(t\right)+\frac{1}{r}\frac{\partial}{\partial r}\left(r\frac{\partial v_0}{\partial r}\right)-\left(M+\frac{1}{K}\right)v_0 \tag{14}$$

$$\frac{\partial v_0}{\partial t} = \frac{1}{r}\frac{\partial}{\partial r}\left(r\frac{\partial v_1}{\partial r}\right)-\left(M+\frac{1}{K}\right)v_1 \tag{15}$$

Where $h\left(t\right) = B\cos\left(\omega t+\theta\right)+B'\cos\beta+\left(1+\varepsilon_0\cos t\right)$.

The corresponding boundary conditions are as under:

$$v_0 = V_s,\ v_1 = 0 \text{ at } r = R \tag{16}$$

$$\frac{\partial v_0}{\partial r} = 0,\ \frac{\partial v_1}{\partial r} = 0 \text{ at } r = 0 \tag{17}$$

The solution of the equations (14), (15) subject to the boundary conditions (16), (17) are as under:

$$v_0 = \left[c_1 J_0\left(r i\sqrt{M+\frac{1}{K}} \right) + \frac{4}{\left(M+\frac{1}{K}\right)} \right] h(t), \quad \text{where} \quad c_1 = \frac{\left[\frac{V_s}{h(t)} - \frac{4}{\left(M+\frac{1}{K}\right)} \right]}{J_0\left(Ri\sqrt{\left(M+\frac{1}{K}\right)} \right)},$$

$v_1 = V(r)h'(t)$, where $h'(t)$ represents the derivative of $h(t)$ with respect to t;

$V(r)$

$$= c_1 J_0\left(r i\sqrt{\left(M+\frac{1}{K}\right)} \right) \left[\frac{r^2}{4} + \psi(r) + \frac{4}{\left(M+\frac{1}{K}\right)^2 c_1 J_0\left(Ri\sqrt{\left(M+\frac{1}{K}\right)} \right)} - \frac{R^2}{4} - \psi(R) \right] - \frac{4}{\left(M+\frac{1}{K}\right)^2}$$

Where, $\psi(r) = \frac{1}{2}\int_0^r x \frac{J_1^{\,2}\left(xi\sqrt{\left(M+\frac{1}{K}\right)} \right)}{J_0^{\,2}\left(xi\sqrt{\left(M+\frac{1}{K}\right)} \right)} dx$.

Consequently, the non-dimensional axial velocity $u(z,r,t)$ is given by:

$u(z,r,t) = v_0(z,r,t) + \varepsilon^2 v_1(z,r,t)$.

3.1 Non-dimensional Wall Shear Stress

Assuming the constricted wall of this artery to be rigid, the non-dimensional wall shear stress τ at $r = R$ is given by:

$$\tau = \frac{2\bar{\tau}}{P_0 \bar{L}},$$

Where $\bar{\tau} = -\upsilon\rho\left(\frac{\partial \bar{u}}{\partial \bar{r}}\right)_{\bar{r}=\bar{R}}$ is the dimensional wall shear stress at $\bar{r} = \bar{R}$.

Consequently, we get:

$$\tau = -\frac{1}{2}\left(\frac{\partial u}{\partial r}\right)_{r=R} = -\frac{1}{2}\left[\left(\frac{\partial v_0}{\partial r}\right)_{r=R} + \varepsilon^2\left(\frac{\partial v_1}{\partial r}\right)_{r=R}\right] \text{ , where}$$

$$\left(\frac{\partial v_0}{\partial r}\right)_{r=R} = -h(t)c_1 i\sqrt{\left(M+\frac{1}{K}\right)}J_1\left(Ri\sqrt{\left(M+\frac{1}{K}\right)}\right),$$

$$\left(\frac{\partial v_1}{\partial r}\right)_{r=R} = h'(t)\left[\frac{R}{2}c_1 J_0\left(Ri\sqrt{M+\frac{1}{K}}\right)\left\{1+\frac{J_1^{\,2}\left(Ri\sqrt{M+\frac{1}{K}}\right)}{J_0^{\,2}\left(Ri\sqrt{M+\frac{1}{K}}\right)}\right\}\right.$$

$$\left. - \frac{4i\sqrt{\left(M+\frac{1}{K}\right)}\,J_1\left(Ri\sqrt{M+\frac{1}{K}}\right)}{\left(M+\frac{1}{K}\right)^2 J_0\left(Ri\sqrt{M+\frac{1}{K}}\right)}\right].$$

3.2 Non-dimensional Volumetric Flow Rate

The dimensionless volumetric flow rate $Q(z,t)$ may be defined as under:

$Q(z,t) = \frac{8\upsilon\rho\,\bar{Q}(\bar{z},\bar{t})}{\pi \bar{L}^4 P_0}$, where $\bar{Q}(\bar{z},\bar{t})$ is the dimensional volumetric flow rate and is given by $\bar{Q}(\bar{z},\bar{t}) = 2\pi\int_0^{\bar{R}} \bar{r}\,\bar{u}(\bar{z},\bar{r},\bar{t})\,d\bar{r}$.

Consequently, $Q(z,t) = 4\int_0^R r\,u(z,r,t)\,dr = I_0 + I_1$, where,

$$I_0 = 4\int_0^R r\, v_0(z, r, t)\, dr = \frac{4h(t)}{\left(M+\frac{1}{K}\right)}\left[2R^2 - c_1 Ri\sqrt{\left(M+\frac{1}{K}\right)}\, J_1\left(Ri\sqrt{M+\frac{1}{K}}\right)\right],$$

$$I_1 = 4\varepsilon^2\int_0^R r\, v_1(z, r, t)\, dr$$

$$= \frac{4\varepsilon^2 h'(t)}{\left(M+\frac{1}{K}\right)}\left[\left\{ - \frac{c_1 R^3 i\sqrt{\left(M+\frac{1}{K}\right)}}{4} - c_1 Ri\sqrt{\left(M+\frac{1}{K}\right)}\,\psi(R)\right.\right.$$

$$\left.\left. - c_1 c_2 Ri\sqrt{\left(M+\frac{1}{K}\right)}\right\} J_1\left(Ri\sqrt{\left(M+\frac{1}{K}\right)}\right) + \frac{c_1 R^2}{2} J_2\left(Ri\sqrt{\left(M+\frac{1}{K}\right)}\right)\right.$$

$$\left. - \frac{2R^2}{\left(M+\frac{1}{K}\right)} + \frac{c_1 i\sqrt{\left(M+\frac{1}{K}\right)}}{2}\int_0^R \frac{r^2 J_1^3\left(ri\sqrt{\left(M+\frac{1}{K}\right)}\right)}{J_0^2\left(ri\sqrt{\left(M+\frac{1}{K}\right)}\right)} dr\right],$$

Where $c_2 = \dfrac{4}{\left(M+\frac{1}{K}\right)^2 c_1 J_0\left(Ri\sqrt{\left(M+\frac{1}{K}\right)}\right)} - \dfrac{R^2}{4} - \psi(R).$

3.3 Non-dimensional Effective Viscosity

Following Pennington and Cowin [28], the effective viscosity $\overline{\mu}_E$ in dimensional form may be expressed as follows:

$$\overline{\mu}_E = \frac{\pi\left(-\dfrac{\partial \overline{P}\left(\overline{z},\overline{t}\right)}{\partial \overline{z}}\right)\left(\overline{R}\left(\overline{z}\right)\right)^4}{\overline{Q}\left(\overline{z},\overline{t}\right)} \Rightarrow \mu_E = \frac{\left(1+\varepsilon_0\cos t\right)R^4}{Q(z,t)}$$

Where μ_E is the non-dimensional effective viscosity.

4 Results and Discussion

In order to get an insight into the biological and physical aspects of this problem, we obtain the profiles of the axial velocity, wall shear stress, volumetric flow rate and the effective viscosity, and we examine their behaviors under the influence of the various non-dimensional parameters relevant to this problem. The data-tabulation involved in this problem is carried out with the aid of Python(x, y) v2.7.6.0, using the packages: cmath, mpmath and numpy. For all the figures, we take $z = 0.2$, $d_0 = 0.3$, $\varepsilon = 0.2$ and $\theta = \frac{\pi}{3}$. Clearly, $r \in [0, R]$ and using (9) and then noting that $|z| < d_0$ for the aforementioned choice of z, d_0, we find that $R = 0.9375$. Thus, for our choice of z, d_0, $r \in [0,\ 0.9375]$.

The Figures 1, 2, 3 and 4 demonstrate the nature of the non-dimensional axial velocity u against r, under the effect of $M, V_s, t, \beta, B, B', \omega, \varepsilon_0$ and K. It is inferred that u decreases as each of M, β, B and ω increases whereas a rise in each of V_s, B', ε_0 and K leads to an increase in u. Also, from Figure 2, it is observed that as t increases from $t = 1$ to $t = 5$ i.e. as ωt rises from $\omega t = \frac{\pi}{4}$ to $\omega t = \frac{5\pi}{4}$, u increases. However, as t further increases from $t = 5$ to $t = 8$ i.e. as ωt further rises from $\omega t = \frac{5\pi}{4}$ to $\omega t = \frac{8\pi}{4}$, u decreases. From (8), we note that $\omega t = \overline{\omega}_0 \bar{t}$. Hence, u rises and then falls with the change in the period of the body acceleration $\overline{F}(\bar{t})$. From all the above mentioned figures it is obvious that the velocity is greatest on the axis ($r = 0$) and least at the stenosed wall ($r = R$). As r increases within $[0, R]$, u decreases from some maximum value at the axis and attains the dimensionless slip velocity $u = V_s$ at the stenosed wall.

The behaviours of dimensionless wall shear stress τ versus time parameter

t under the effects of the parameters $M, V_s, \beta, B, B', \omega, \varepsilon_0, d_s$ and K are depicted in the figures 5, 8 and 9. It is noted that the wall shear stress falls with the rise in each of M, V_s, β, ω and d_s. On the other hand, the shear stress exhibits a growth with the increase in each of B', ε_0 and K. However, a growth in B causes τ to initially rise for smaller values of t and then decrease for comparatively larger values of t. This may be attributed to the periodic nature of the body acceleration as well as the pressure gradient.

The profiles for the non-dimensional volumetric flow rate Q against time parameter t under the influence of the parameters $M, V_s, \beta, B, B', \omega, \varepsilon_0, d_s$ and K are demonstrated in the figures 6, 10 and 11. It is observed that the volumetric flow rate registers a drop with the growth in each of M, β, ω and d_s. But an augmentation in each of V_s, B' and K leads to a corresponding increase in Q. Also, a rise in each of B and ε_0 causes Q to rise for relatively smaller values of t and then leads Q to fall for comparatively larger values of t. This is attributable to the periodic nature of the body acceleration and the pulsatile nature of the pressure gradient.

The effects of the quantities M, V_s, β, B, B', ω, ε_0, d_s and K on the dimensionless effective viscosity μ_E against time t are depicted in the Figures 7, 12 and 13. Clearly, μ_E exhibits a growth with a rise in each of M, β and ω. However, an increase in each of V_s, B', K and d_s leads to a fall in μ_E. Moreover, an augmentation in B causes μ_E to decrease for smaller values of t and then leads to an increase for relatively larger values of t. This is due to the periodic body acceleration and the pulsatile pressure gradient. Furthermore, a growth in ε_0 causes μ_E to increase for smaller values of t and then leads to a decrease for moderate values of t. Thereafter, for comparatively larger values of t, μ_E again registers a growth as ε_0 increases. This is due to the pulsatile

nature of the pressure gradient.

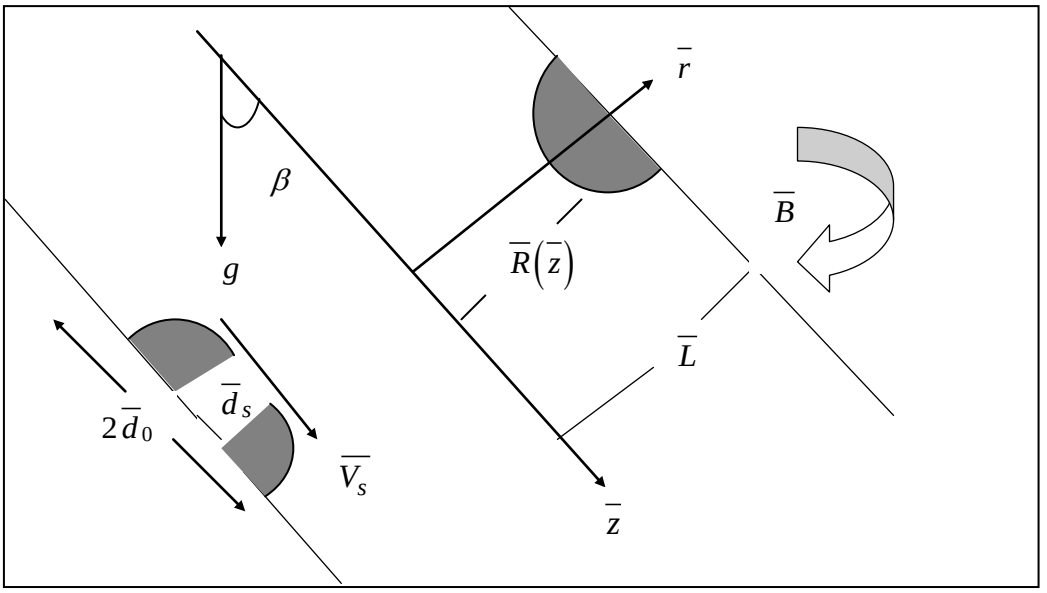

Schematic figure of an inclined stenosed artery with azimuthal magnetic field

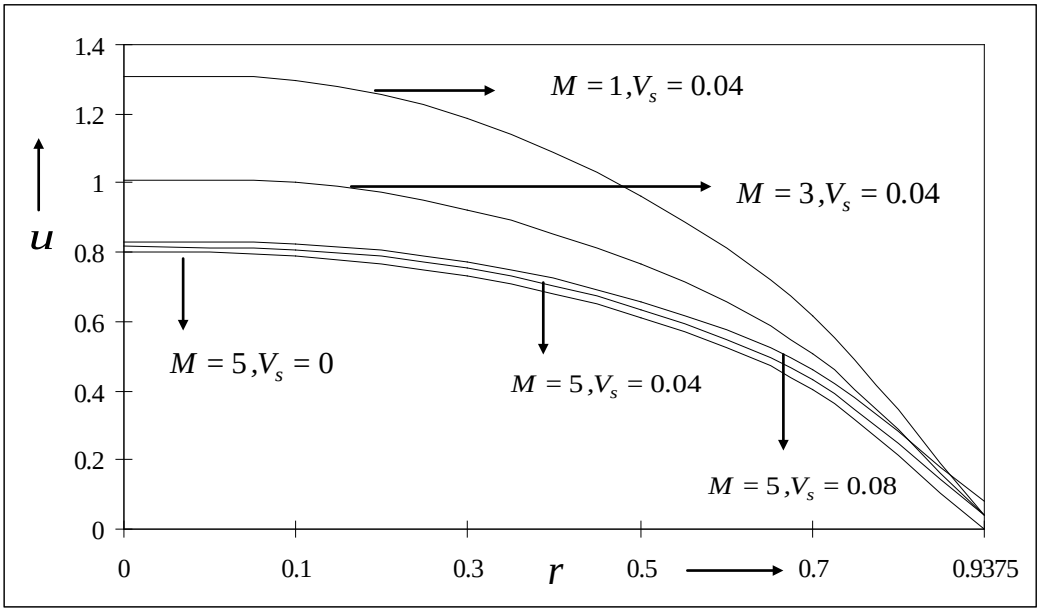

Figure 1: Velocity u against r, under the effect of M and V_s for $K \to \infty$

$d_s = 0.25,\ R = 0.9375,\ t = 1,\ \omega = \frac{\pi}{4},\ \varepsilon_0 = 0.8,\ B = 0.8,\ \beta = \frac{\pi}{8},\ B' = 0.5$

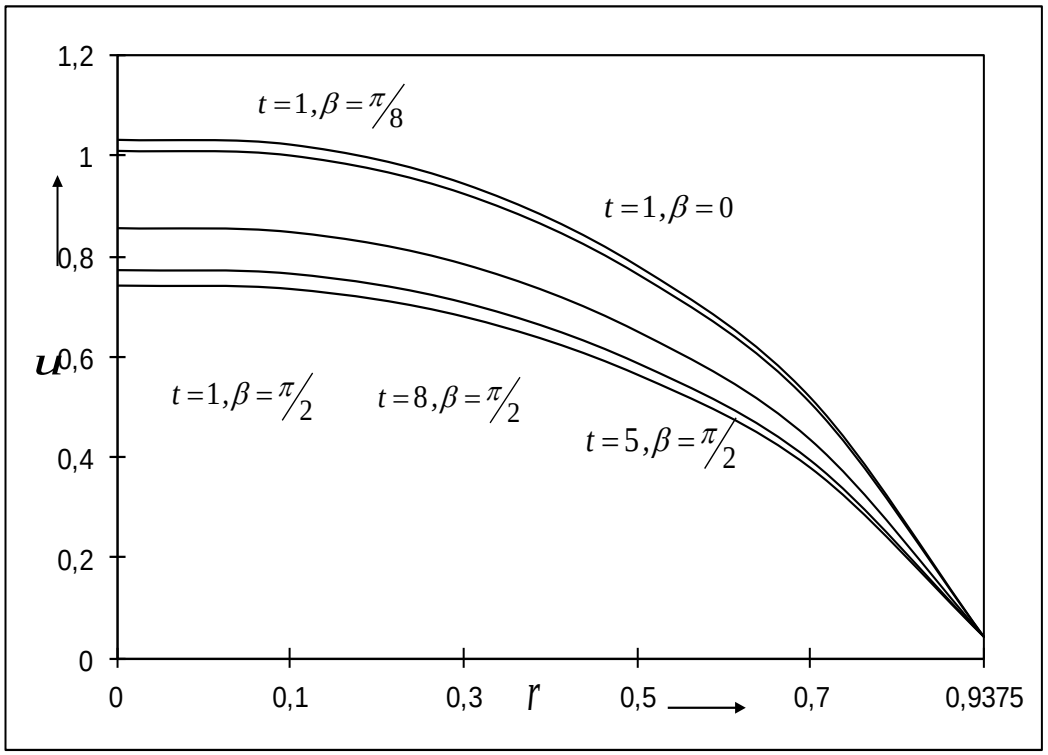

Figure 2: Velocity u against r, under the effect of t and β for $K \to \infty$

$d_s = 0.25,\ R = 0.9375,\ M = 3,\ \omega = \frac{\pi}{4},\ \varepsilon_0 = 0.8,\ B = 0.8,\ V_s = 0.04,\ B' = 0.5$

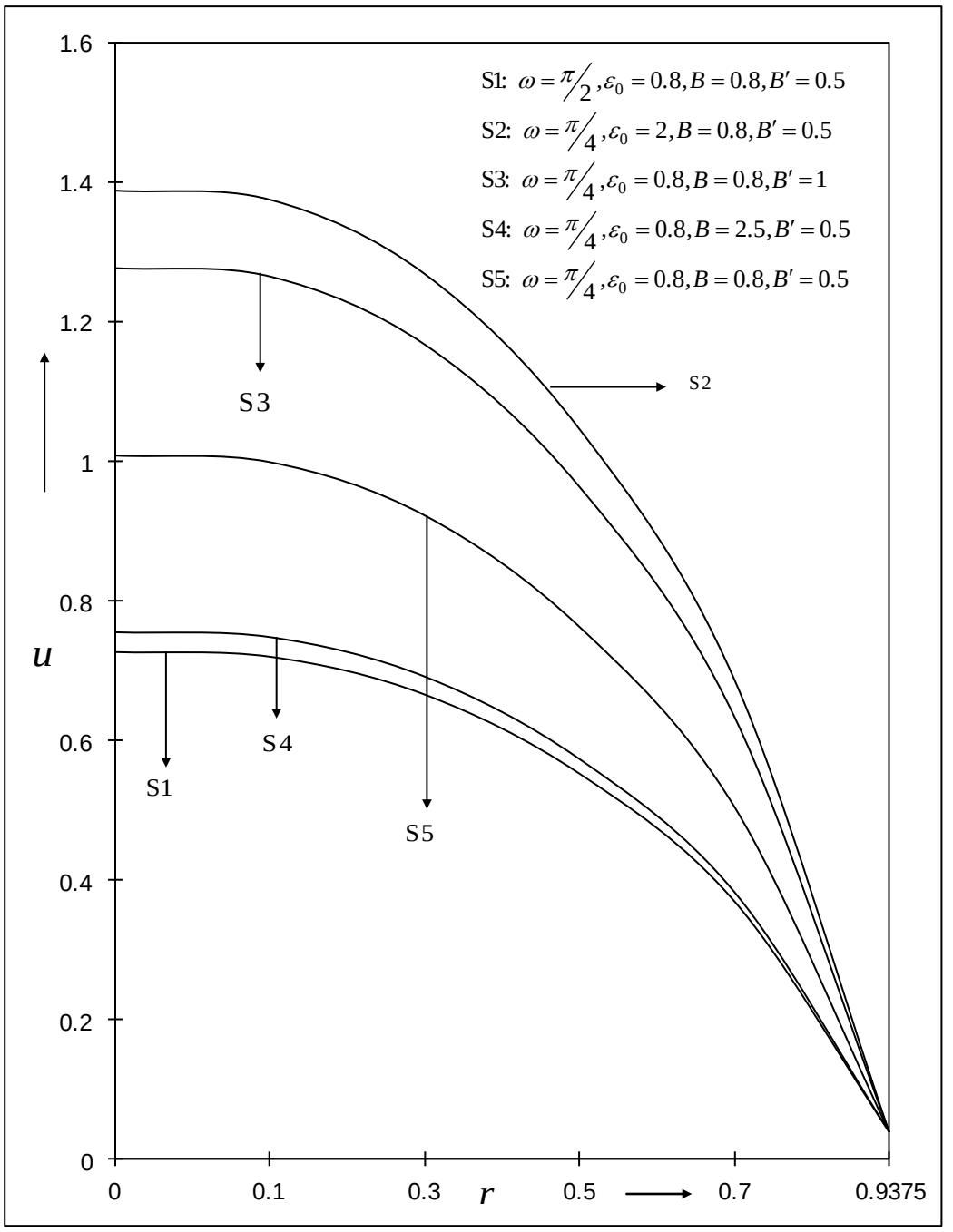

Figure 3: Velocity u against r, under the effect of B, B', ω and ε_0 for $d_s = 0.25,\ R = 0.9375,\ M = 3,\ V_s = 0.04,\ t = 1, K \to \infty$

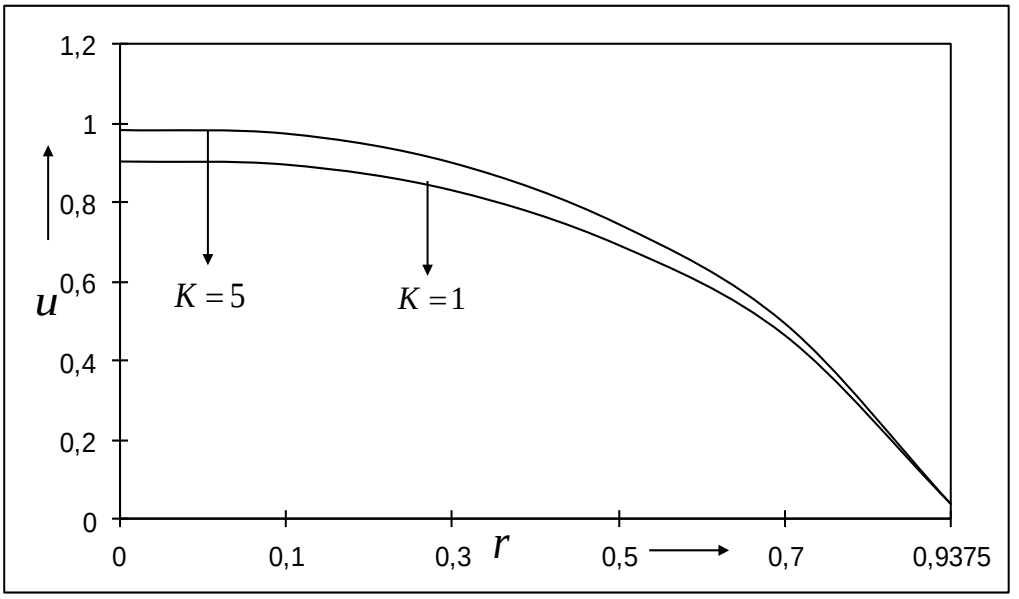

Figure 4: Velocity u against r, under the effect of K for $M = 3, B = 0.8,$

$d_s = 0.25,\ R = 0.9375,\ t = 1,\ V_s = 0.04,\ \omega = \pi/4,\ \varepsilon_0 = 0.8,\ \beta = \pi/8,\ B' = 0.5$

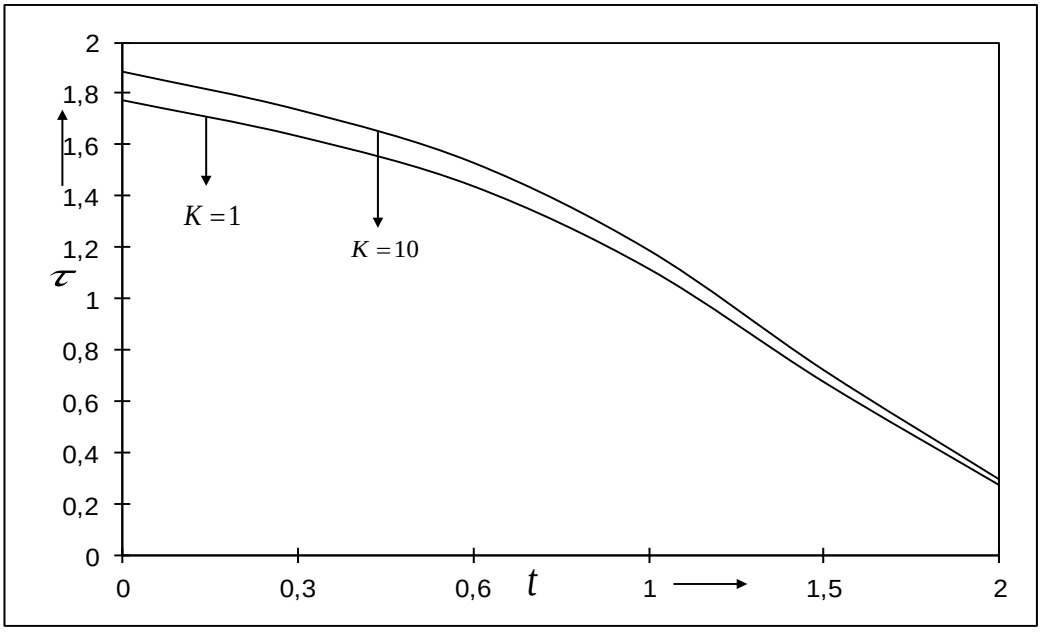

Figure 5: Shear stress τ against t, under the effect of K for $V_s = 0.04,$

$d_s = 0.25,\ \varepsilon_0 = 0.8,\ B = 0.8,\ B' = 0.5,\ \omega = \dfrac{\pi}{4}, M = 3,\ \beta = \pi/8$

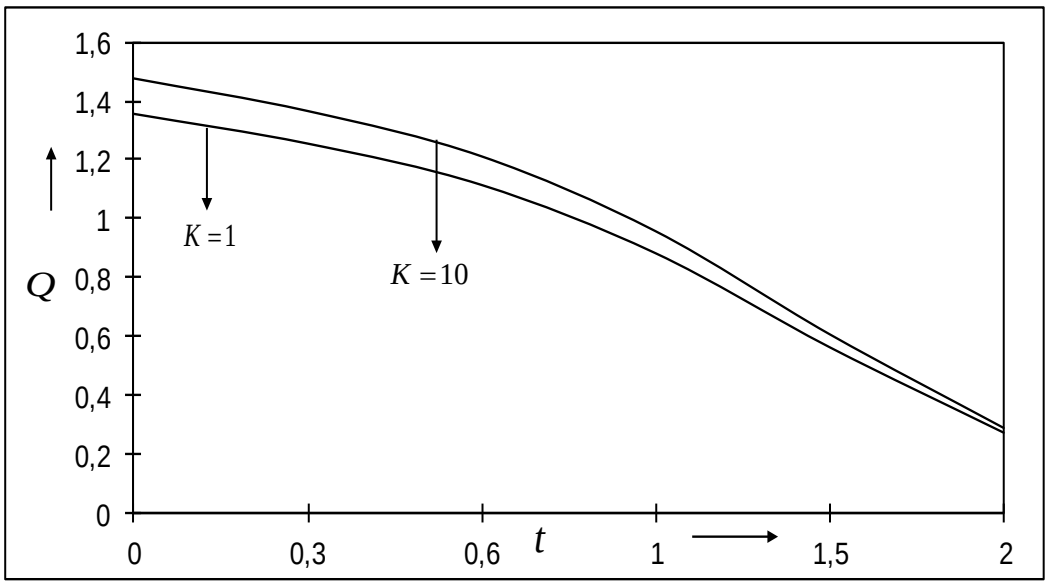

Figure 6: Flow rate Q against t, under the effect of K for $V_s = 0.04$, $d_s = 0.25$, $\varepsilon_0 = 0.8$, $B = 0.8$, $B' = 0.5$, $\omega = \frac{\pi}{4}$, $M = 3$, $\beta = \pi/8$

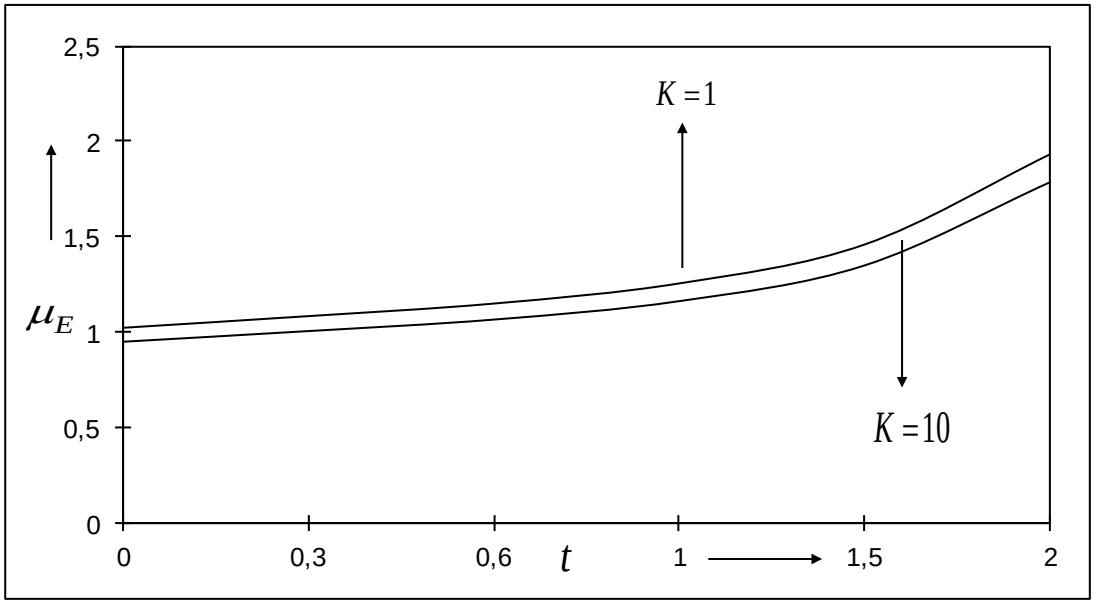

Figure 7: Effective viscosity μ_E against t, under the effect of K for $V_s = 0.04$, $d_s = 0.25$, $\varepsilon_0 = 0.8$, $B = 0.8$, $B' = 0.5$, $\omega = \frac{\pi}{4}$, $M = 3$, $\beta = \pi/8$

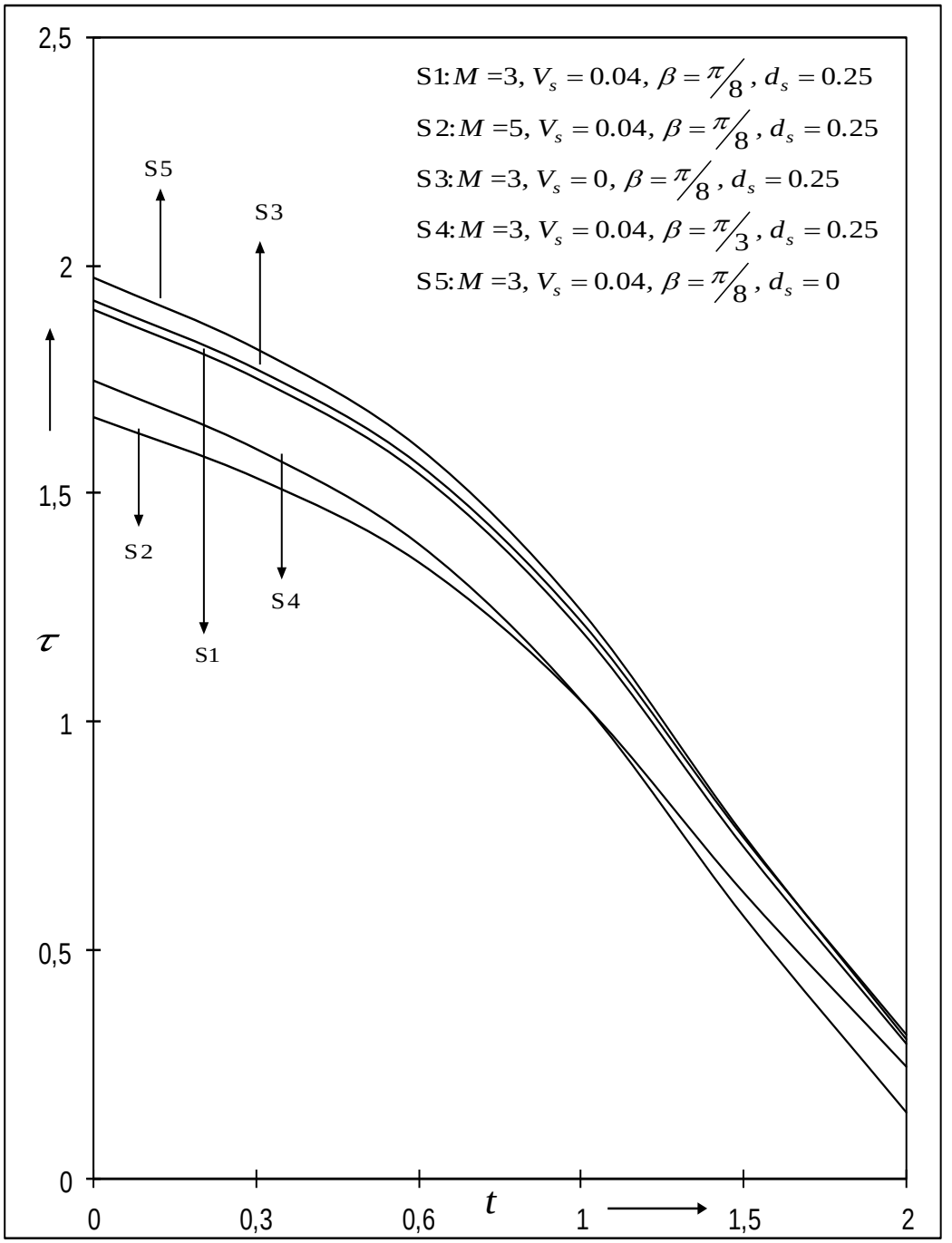

Figure 8: Shear stress τ against t, under the effect of M, V_s, β and d_s for $\varepsilon_0 = 0.8,\ B = 0.8,\ B' = 0.5,\ \omega = \dfrac{\pi}{4},\ K \to \infty$

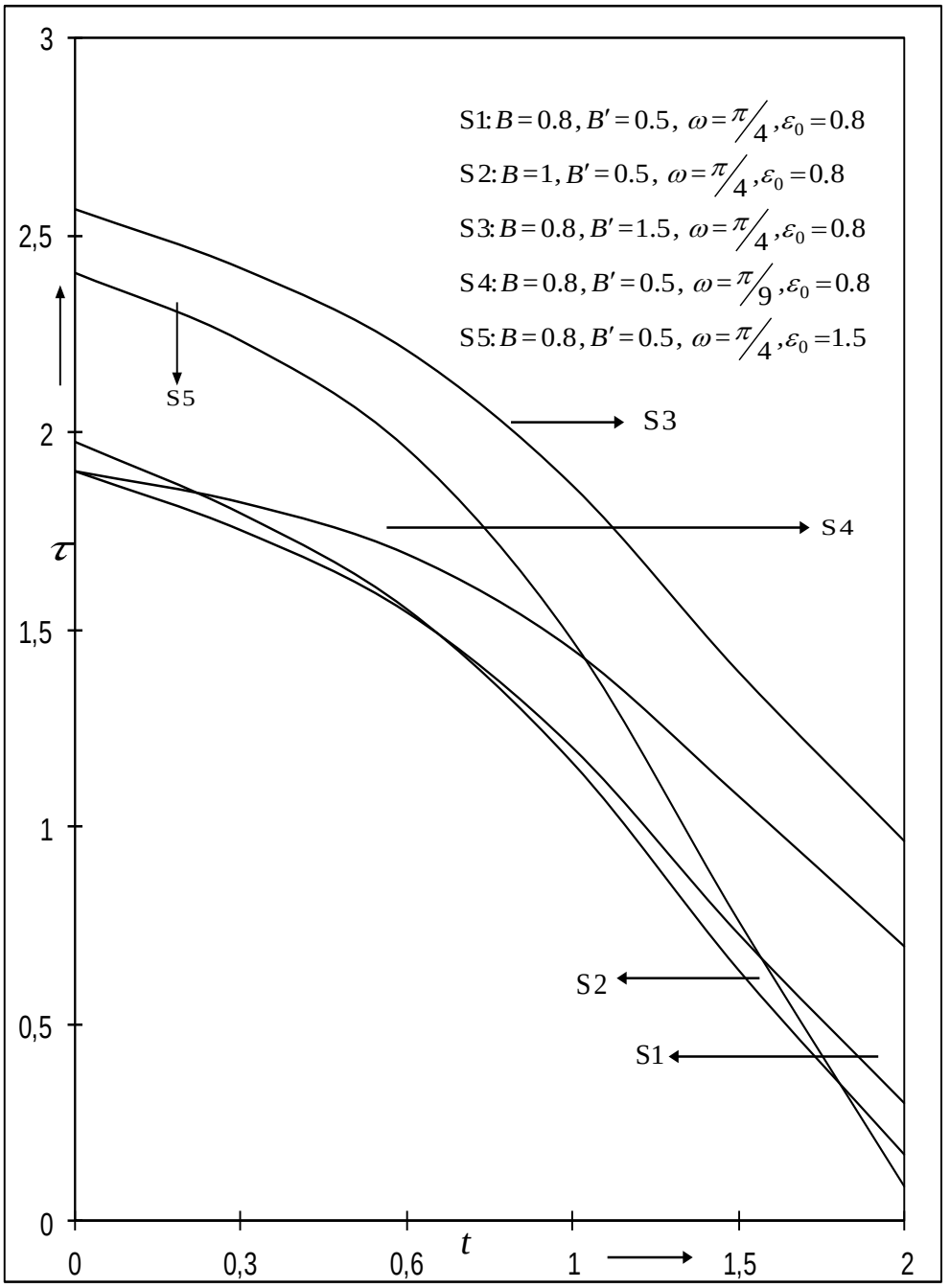

Figure 9: Shear stress τ against t, under the effect of B, B', ω and ε_0 for $M=3,\ V_s=0.04,\ d_s=0.25,\ \beta=\dfrac{\pi}{8},\ K\to\infty$

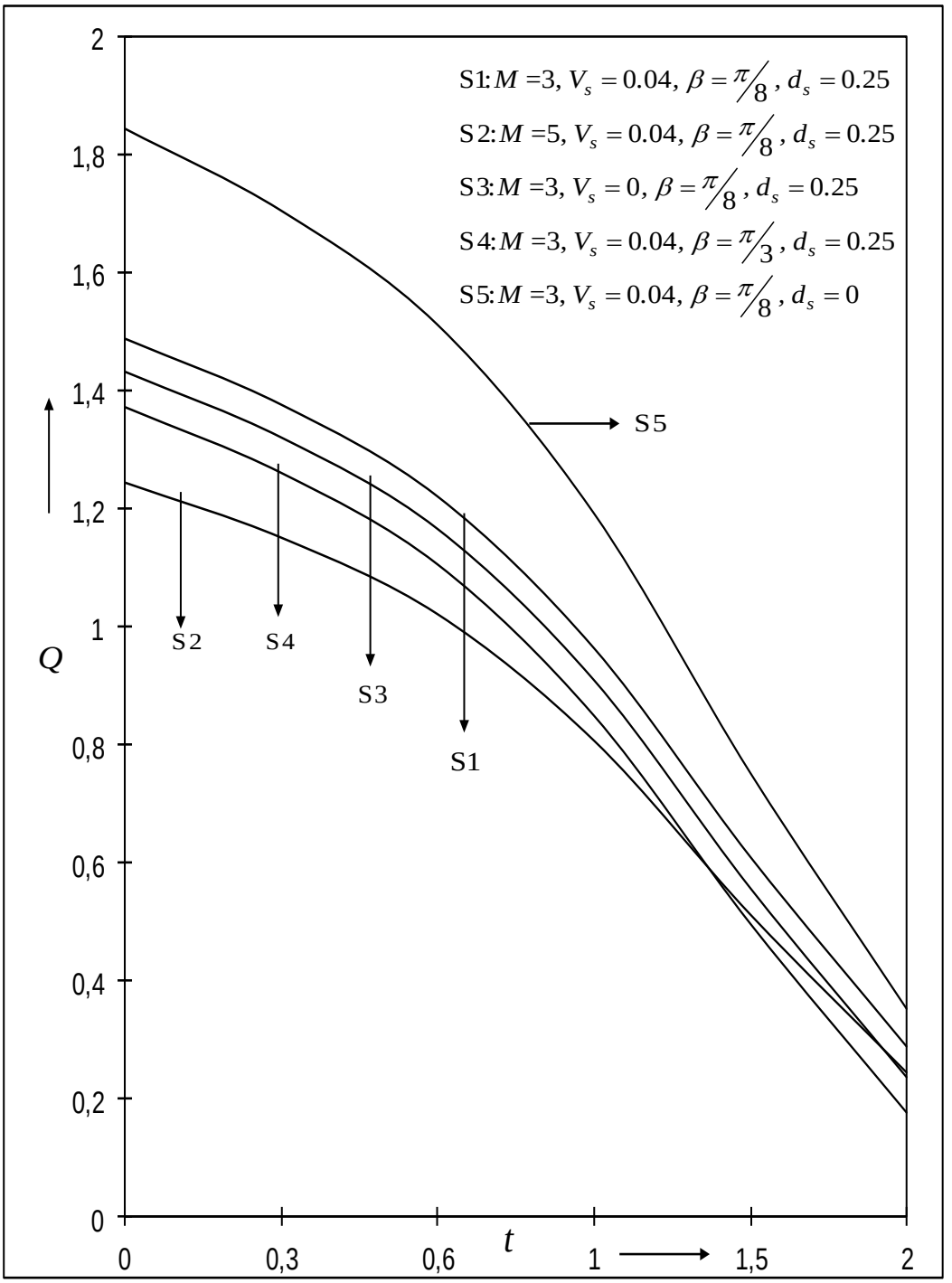

Figure 10: Flow rate Q against t, under the effect of M, V_s, β and d_s for $\varepsilon_0 = 0.8,\ B = 0.8,\ B' = 0.5,\ \omega = \dfrac{\pi}{4},\ K \to \infty$

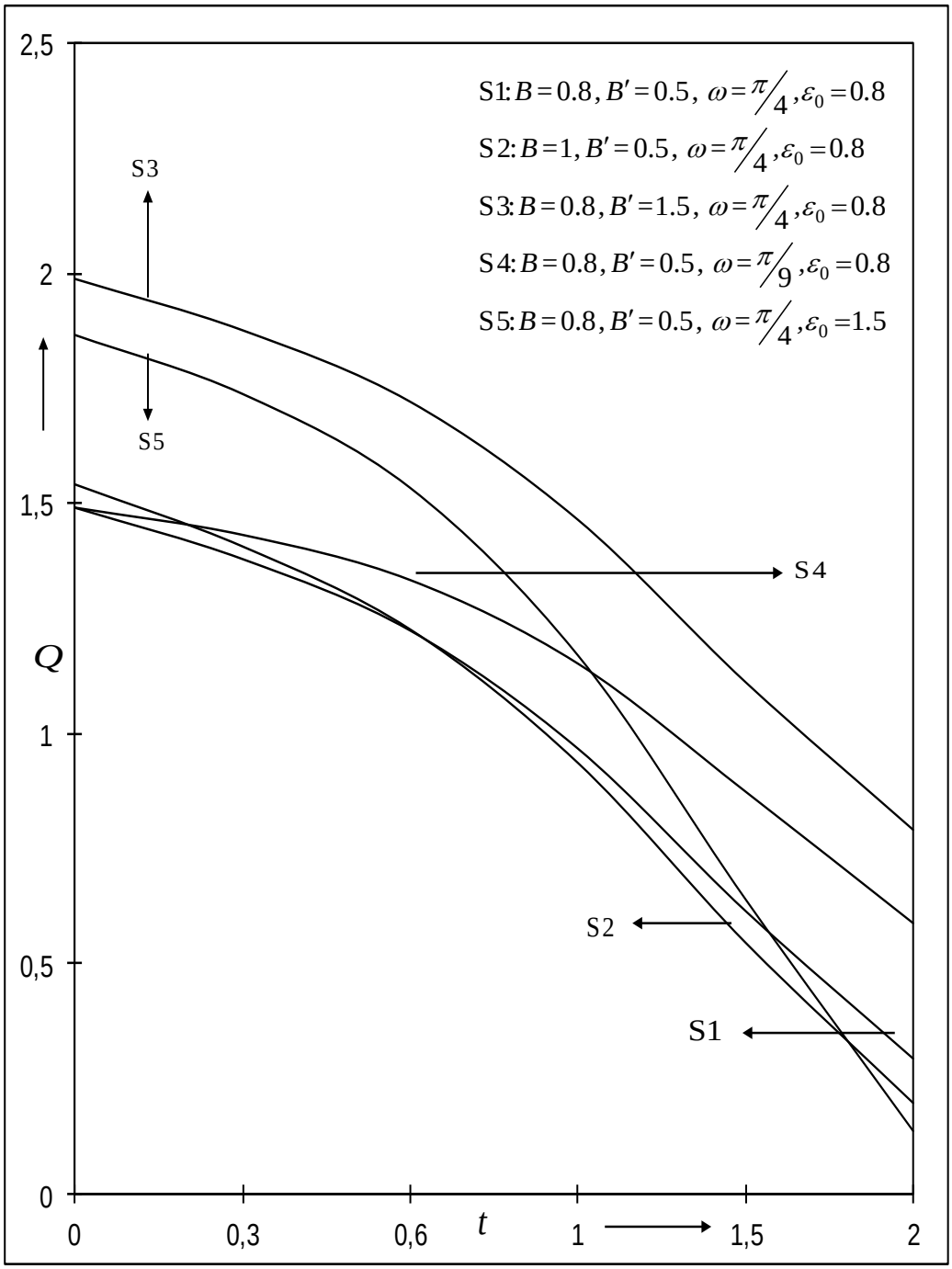

Figure 11: Flow rate Q against t, under the effect of B, B', ω and ε_0 for $M=3,\ V_s=0.04,\ d_s=0.25,\ \beta=\dfrac{\pi}{8},\ K\to\infty$

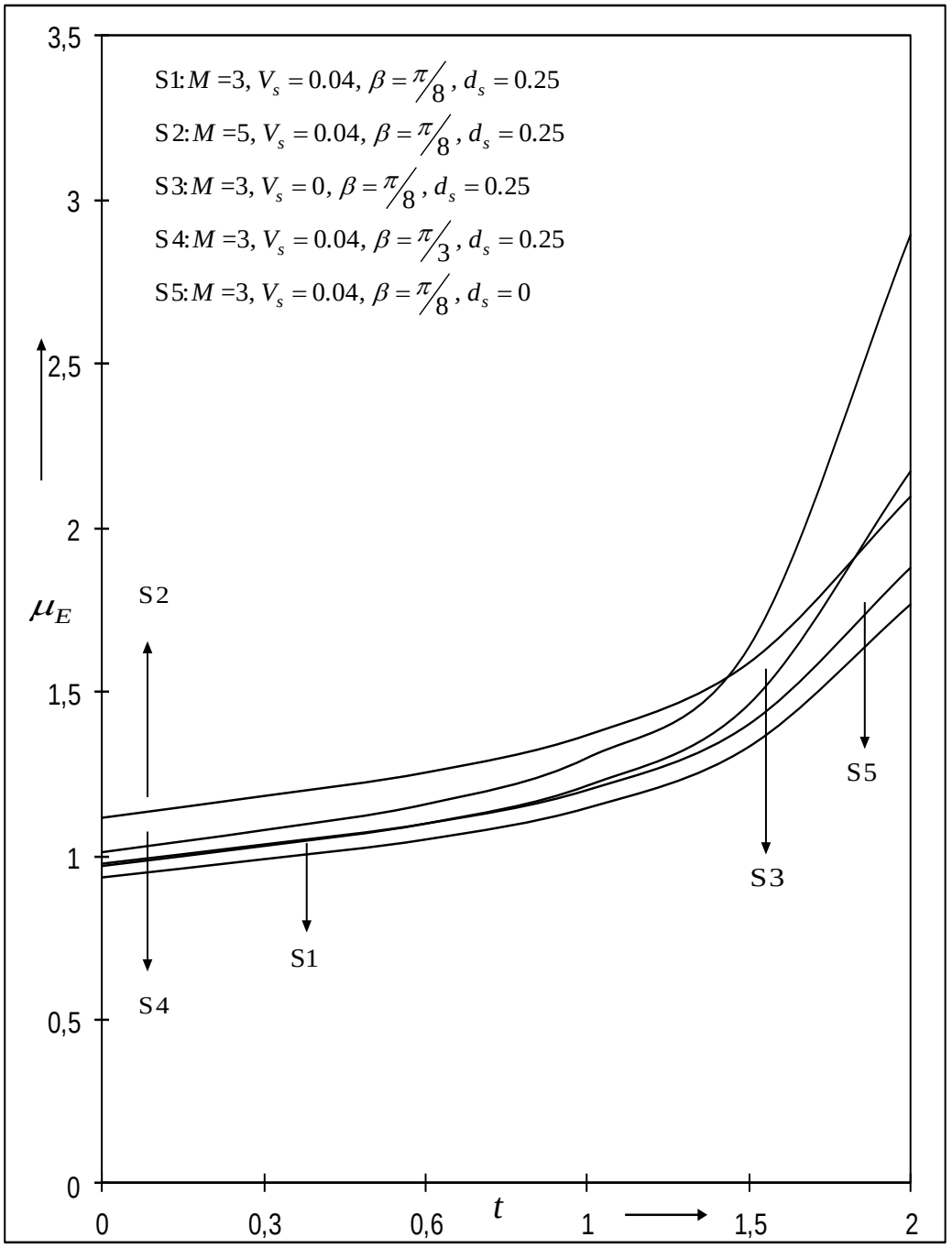

Figure 12: Effective viscosity μ_E against t, under the effect of M, V_s, β, d_s for $\varepsilon_0 = 0.8,\ B = 0.8,\ B' = 0.5,\ \omega = \dfrac{\pi}{4},\ K \to \infty$

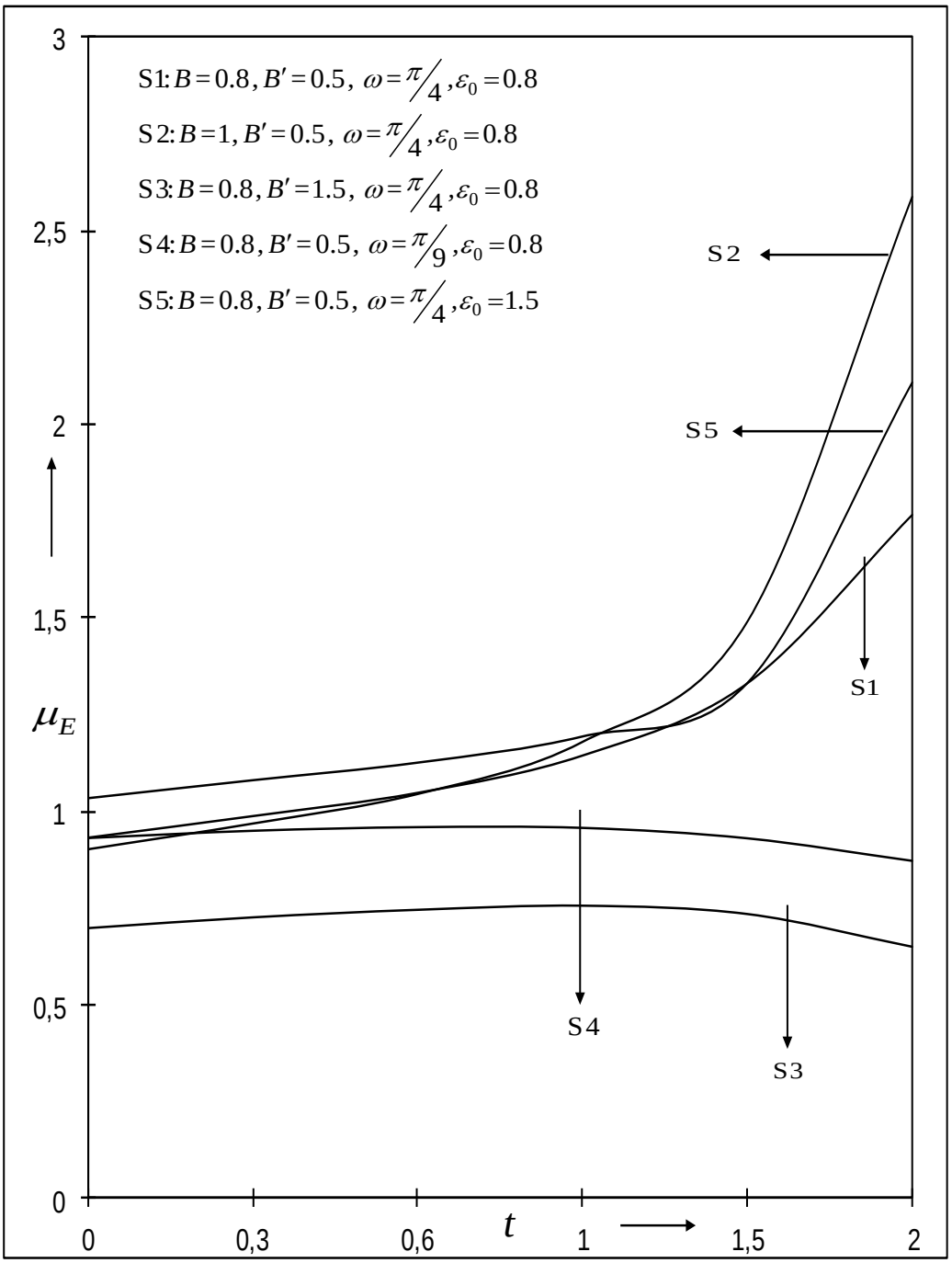

Figure 13: Variation of effective viscosity μ_E against t, under the effect of $B,\ B', \omega,\ \varepsilon_0$ for $M=3, V_s=0.04,\ d_s=0.25,\ \beta=\dfrac{\pi}{8},\ K\to\infty$

5 Conclusion

In view of the above flow model and the subsequent observations, we arrive at the following conclusions:

[5.1] For this inclined artery, the imposition of the magnetic field causes a decrease in each of axial velocity of blood, wall shear stress and the volumetric flow rate. But the effective viscosity of blood rises as the magnetic field increases. This shows that the applied azimuthal magnetic has considerable scope in the field of treating cardiovascular diseases resulting from stenosis. The use of an azimuthal magnetic field can aid in effectively controlling the blood velocity and minimizing the large shear stress on the stenosed arterial wall. The axial velocity profiles are parabolic in shape.

[5.2] In case of this inclined artery, the imposition of the slip velocity leads to a growth in each of axial velocity of blood and the volumetric flow rate. Thus, the blood flow rate is enhanced. But, the wall shear stress and the effective viscosity decrease with the imposition of the slip velocity. Hence, slip inducing medical drugs may be beneficial in effectively controlling the wall shear stress and the effective viscosity of blood in a stenosed artery.

[5.3] As the angle of inclination increases, the blood velocity, the wall shear stress and the volumetric flow rate decrease whereas the effective viscosity increases.

[5.4] In this inclined artery, a rise in the permeability of the medium causes each of axial blood velocity, wall shear stress and the volumetric flow rate to increase and the effective viscosity to decrease. In certain pathological conditions, the distribution of fatty cholesterol and artery-clogging blood clots in the lumen of the coronary artery may be represented by a fictitious porous medium. Therefore, an augmentation in the permeability of such porous media can enhance the blood flow rate in a stenosed artery. This may be achieved through the development of proper medical procedures and by

developing medical drugs that enhance the permeability in a stenosed / clogged artery.

[5.5] In the inclined artery, a growth in the height of arterial stenosis causes a corresponding decrease in each of wall shear stress at the stenosed region of the arterial wall, blood flow rate and the effective viscosity. Hence, the blood flow rate in the stenosed artery may be enhanced by reducing the height of stenosis i.e. by unblocking clogged arteries. This again calls for developing suitable medical procedures and medical drugs.

[5.6] As B (relative effectiveness of the periodic body acceleration to the pulsatile pressure gradient) rises, the axial blood flow velocity decreases. But the wall shear stress and the volumetric flow rate initially increase and then again decrease, as B increases. However, the effective viscosity initially drops and then again rises, with the augmentation in B. The fluctuating trends in case of shear stress, the flow rate and the effective viscosity are attributable to the periodic body acceleration and the pulsatile pressure gradient. Patients with cardiovascular problems should avoid situations demanding excessive body accelerations.

[5.7] Each of axial blood velocity, shear stress and blood flow rate exhibits a growth whereas the effective viscosity registers a drop as B' (relative effectiveness of body force per unit volume of blood to the pulsatile pressure gradient) increases. Therefore, an increase in the total blood volume may lead to increased arterial wall shear stress.

[5.8] Each of axial blood velocity, shear stress and blood flow rate registers a fall whereas the effective viscosity exhibits a rise with the rise in ω (relative effectiveness of the frequency of body acceleration to the pulse rate frequency).

[5.9] A rise in ε_0 (relative effectiveness of the amplitude of the oscillatory part of pressure gradient to the steady state pressure gradient) leads to an augmentation in axial blood velocity and the shear stress. On the other hand,

due to a rise in ε_0, the volumetric flow rate and the effective viscosity exhibit an increasing and a decreasing trend versus time. This is due to the pulsatile nature of the pressure gradient.

It may be noted that the above results and the ensuing conclusions are presented under the selected range of data.

ACKNOWLEDGEMENTS. The authors are highly thankful to CSIR-HRDG for funding this research work under Research Grant-in-aid No. 25(0209)/12/EMR-II.

References

[1] Y. C. Fung, *Biodynamics Circulation*, Springer-Verlag, New York, 1984.

[2] D. A. McDonald, *Blood Flow in Arteries*, Arnold, London, 1960.

[3] M. Zamir, *The Physics of Coronary Blood Flow*, Springer, New York, 2005.

[4] M.W. David, P.M. Christos, R.H. Stephen and N. Ku. David, A mechanistic model of acute platelet accumulation in thrombogenic stenoses, *Annals of Biomedical Engineering*, **29**(4), (2001), 321-329.

[5] D.F. Young, Fluid Mechanics of Arterial Stenoses, *Journal of Biomechanical Engineering*, **101**, (1979), 157-175.

[6] Z. R. Liu, G. Xu, Y. Chen, Z. Z. Teng and K. R. Qin, An Analysis Model of Pulsatile Blood Flow in Arteries, *Applied Mathematics and Mechanics*, **24**, (2003), 230-240.

[7] L. Yao and D. Z. Li, Pressure and Pressure Gradient in an Axisymmetric Rigid Vessel with Stenosis, *Applied Mathematics and Mechanics*, **27**, (2006), 347-351.

[8] Kh. S. Mekheimer and M. A. El Kot, Influence of Magnetic Field and Hall Currents on Blood Flow through a Stenotic Artery, *Applied Mathematics and Mechanics*, **29**, (2008), 1093-1104.

[9] V. K. Sud and G. S. Sekhon, Blood flow subject to a single cycle of body acceleration, *Bulletin of Mathematical Biology*, **46**, (1984), 937-949.

[10] M. El-Shahed, Pulsatile flow of blood through a stenosed porous medium under periodic body acceleration, *Appl. Math. Comput.*, **138**, (2003), 479-488.

[11] E.F. Elshehawey, E.M.E. Elbarbary, M.E. Elsayed, N.A.S. Afifi and M. El-Shahed, Pulsatile flow of blood through a porous medium under periodic body acceleration, *Int. J. Theoretical Phys*., **39**(1), (2000), 183-188.

[12] P. Brunn, The Velocity Slip of Polar Fluids, *Rheol. Acta*., **14**, (1975), 1039-1054.

[13] A.L. Jones, On the Flow of Blood in a Tube, *Biorheology*, **3**, (1966), 183-188.

[14] L. Bennet, Red Cell Slip at a Wall, *in vitro*. *Science*, **155**, (1967), 1554-1556.

[15] G. Bugliarello and J. W. Hayden, High Speed Micro Cinematographic Studies of Blood Flow, *in vitro*. *Science*, **138**, (1962), 981-983.

[16] G. Astarita and G. Marrucci, *Principles of Non-Newtonian Fluid Mechanics*, McGraw-Hill, New York, USA, 1974.

[17] D. C. H. Cheng, The Determination of Wall Slip Velocity in the Laminar Gravity Flow of Non-Newtonian Fluids along Plane Surfaces, *Ind. Eng. Chem. Fundamen*., **13**, (1974), 394-395.

[18] A. Kolin, An Electromagnetic Flowmeter: Principle of Method and Its Application to Blood Flow Acceleration, *Experimental Biology and Medicine*, **35**, (1936), 53-56.

[19] E. M. Korchevskii and L. S. Marochnik, Magneto Hydrodynamic Version of Movement of Blood, *Biophysics*, **10**, (1965), 411-413.

[20] M. F. Barnothy, *Biological Effects of Magnetic Fields*, Plenum Press, New York, 1964.

[21] Z. L. Xu, JMu, J. Liu, M. M. Kamocka, X. Liu, D. Z. Chen, E. D. Rosen and M. S. Alber, Multiscale model of venous thrombus formation with surface-mediated control of blood coagulation cascade, *Biophysical Journal*, **98**, (2010), 1723-1732.

[22] Z. L. Xu, N. Chen, M. M. Kamocka, E. D. Rosen and M. S. Alber, Multiscale Model of Thrombus Development, *Journal of the Royal Society Interface*, **4**(24), (2008), 705-723.

[23] Z. L. Xu, N. Chen, S. Shadden, J. E. Marsden, M. M. Kamocka, E. D. Rosen and M. S. Alber, Study of blood flow impact on growth of thrombi using a multiscale model, *Soft Matter*, **5**, (2009), 769-779.

[24] J.T. Ottesen, M.S. Olufsen and J.K. Larsen, Applied Mathematical Models in Human Physiology, *SIAM monographs on mathematical modeling and computation*, (2004).

[25] P. Nagarani and G. Sarojamma, Effect of body acceleration on pulsatile flow of Casson fluid through a mild stenosed artery, *Korea-Australia Rheology Journal*, **20**, (2008), 189-196.

[26] E. F. EL Shehawey and W. E. L. Sebaei, Peristaltic transport in a cylindrical tube through a porous medium, *International Journal of Mathematics and Mathematical Sciences*, **24**, (2000), 217-230.

[27] E.E. Tzirtzilakis, A Mathematical Model for Blood Flow in Magnetic Field, *Physics of Fluids*, **17**, (2005), 1-15.

[28] C. J. Pennington and S. C. Cowin, The Effective Viscosity of Polar Fluids, *Trans. Soc. Rheol*., **14**, (1970), 219-238.